Supplementary Information for

Can satellite and reanalysis estimates capture the intra-annual structure of localised temperature trends? Novel diagnostic metrics and station evidence from a data-sparse tropical region, with implications for climate adaptation

Author names removed for blind review

*Affiliations removed for blind review.

S1 Homogeneity Tests and Homogenisation

Homogeneity testing is a critical pre-processing step that ensures detected temperature trends reflect genuine climatic signals rather than non-climatic artefacts such as station relocations, instrument changes, or shifts in observation practice (Wijngaard et al. 2003). The AgERA5 dataset (Copernicus Climate Change Service 2019) is a curated version of the ERA5 reanalysis tailored for agricultural applications, providing daily temperature data at $0.1^\circ \times 0.1^\circ$ resolution with corrections based on station observations; it served as the homogenisation reference series in this study. The four tests applied and their mathematical definitions are described below.

S1.1 Observational Data Quality Control

Several internal consistency verifications were performed to ensure the integrity of the data. First, we verified that the minimum temperature (Tmin) did not exceed the Tmax for any given day. In instances where this occurred, the values were frequently found to be swapped; such entries were corrected accordingly. In other cases, obvious typographical errors, such as 32.1 written as 23.1, were corrected by cross-referencing adjacent data points. If the discrepancy could not be resolved by these methods, the values were flagged as missing. Threshold verifications were also applied to identify unrealistic extremes. Maximum temperature values exceeding 50°C were investigated, often revealing digit reversals such as 63 instead of 36. Similarly, minimum temperatures below 10°C were examined, revealing decimal placement errors such as 2.4 instead of 24. These were corrected on the basis of the context of neighbouring values.

To address temporal consistency, we monitored large fluctuations between consecutive days and the occurrence of persistent identical values. Inter-diurnal changes in Tmax or Tmin exceeding 10°C were scrutinised for typos or parameter swaps. Furthermore, if a constant value was recorded for more than five consecutive days, those observations were deemed suspicious and marked as missing to avoid biasing the trend analysis.

S1.2 The Standard Normal Homogeneity Test (SNHT)

The Standard Normal Homogeneity Test, as developed by Alexandersson (1986), utilizes a likelihood ratio statistic to compare the mean of the first m years with the mean of the remaining $n - m$ years in a given series Y. The test statistic $T(m)$ is defined as follows:

$$T(m) = m\bar{z}_1^2 + (n-m)\bar{z}_2^2, \quad m = 1, \ldots, n \tag{1}$$

In this equation, the standardized mean values for the two sub-periods are calculated as:

$$\bar{z}_1 = \frac{1}{m}\sum_{i=1}^{m}(Y_i - \bar{Y})/\sigma \quad \text{and} \quad \bar{z}_2 = \frac{1}{n-m}\sum_{i=m+1}^{n}(Y_i - \bar{Y})/\sigma \tag{2}$$

where n is the number of observations in the series, and $\bar{Y}$ and σ represent the mean and sample standard deviation of the entire series, respectively. When a break occurs at year M, the function $T(m)$ reaches its maximum value near $m = M$. The global test statistic T is determined by finding the maximum value across the sequence:

$$T = \max_{1 \le m < n} T(m) \tag{3}$$

The SNHT is a parametric test that assumes the underlying data follows a normal distribution. A primary property of this test is its high sensitivity to shifts occurring at the beginning or the end of a time series. While it is highly effective at detecting abrupt changes in mean, its parametric nature makes it less robust to outliers or non-normal data distributions compared to rank-based methods.

S1.3 Pettitt Test (PT)

The Pettitt test (Pettitt 1979) is a non-parametric approach for change point detection based on the ranks of the observations. This method is particularly useful when the distribution of the data is unknown or non-normal. For a series $Y_1, \ldots, Y_n$, let $r_1, \ldots, r_n$ be the corresponding ranks. The test statistics are computed as follows:

Fig. S1 A plot of the homogeneity test results for SNHT across all the stations. The change point (CP) identifies the year of maximum likelihood for a shift in the mean, with statistical significance denoted by the p at 95% confidence level. Orange and green dashed horizontal lines indicate the mean temperature regimes before and after the detected break, respectively.

$$U_m = 2\sum_{i=1}^{m} r_i - m(n+1), \quad m = 1, \ldots, n \tag{4}$$

If a change point occurs at year M, the statistic U_m reaches either its maximum or minimum value near $m = M$. The final test statistic is the maximum absolute value of U_m:

$$U_M = \max_{1 \leq m \leq n} |U_m| \tag{5}$$

The Pettitt test is recognized for its robustness against outliers because it utilizes ranks rather than the absolute values of the data. Unlike the SNHT, this test is more sensitive to shifts occurring in the middle of a time series and is generally less powerful at identifying changes located near the boundaries of the data record.

S1.4 Buishand's Tests

The assessment of homogeneity in the climate series is based on the calculation of adjusted partial sums and specific test statistics designed to identify shifts in the mean. The adjusted partial sums, denoted as S_m^*, represent the cumulative deviations of the observations from the series mean (Buishand 1984). These are defined as:

$$S_0^* = 0, \quad S_m^* = \sum_{i=1}^{m} (Y_i - \bar{Y}), \quad m = 1, \ldots, n \tag{6}$$

In this expression, Y_i represents the observation at time i and $\bar{Y}$ denotes the sample mean. In a homogeneous series, these sums fluctuate around zero, while a sudden shift in the mean causes the sums to trend upward or downward, typically reaching a peak or trough at the point of change. The internal variability of the dataset is accounted for by the sample standard deviation, σ.

S1.4.1 Buishand likelihood ratio test (BLRT)

To detect an abrupt change at an unknown time, the likelihood ratio statistic V is employed (Buishand 1984). This statistic is defined as:

$$V = \max_{1 \leq m \leq n-1} \left\{ \frac{|S_m^*|}{\sigma \{m(n-m)\}^{1/2}} \right\} \tag{7}$$

The V statistic is particularly effective for identifying shifts that occur near the beginning or the end of a time series (Buishand 1984).

S1.4.2 Buishand's U test (BUT)

The Bayesian statistic U is used to evaluate shifts when the position of the change point is assumed to have a uniform prior distribution (Buishand 1984). The statistic is defined as:

$$U = \frac{1}{n(n+1)} \sum_{m=1}^{n-1} \left(\frac{S_m^*}{\sigma} \right)^2 \tag{8}$$

Unlike the likelihood ratio test, the U statistic gives less weight to the series end-points and is therefore more sensitive to mean shifts occurring in the middle of the sequence (Buishand 1984).

Fig. S2 A plot of the homogeneity test results for PT across all the stations. The change point (CP) identifies the year of maximum likelihood for a shift in the mean, with statistical significance denoted by the p at 95% confidence level. Orange and green dashed horizontal lines indicate the mean temperature regimes before and after the detected break, respectively.

S1.5 Homogenisation Methodology

Tmax and Tmin series were homogenised using the *Climatol* package (Guijarro 2025) in R, with daily AgERA5 fields at the nearest pixel serving as the reference series.

Fig. S3 A plot of the homogeneity test results for BLRT across all the stations. The change point (CP) identifies the year of maximum likelihood for a shift in the mean, with statistical significance denoted by the p at 95% confidence level. Orange and green dashed horizontal lines indicate the mean temperature regimes before and after the detected break, respectively.

Although reanalysis data may contain systematic biases, they are generally considered more spatially and temporally homogeneous than raw station records, making them suitable as homogenisation references (World Meteorological Organization 2021;

Fig. S4 A plot of the homogeneity test results for BUT across all the stations. The change point (CP) identifies the year of maximum likelihood for a shift in the mean, with statistical significance denoted by the p at 95% confidence level. Orange and green dashed horizontal lines indicate the mean temperature regimes before and after the detected break, respectively.

Guijarro 2025); in a data-sparse tropical region where no dense neighbouring station network is available, a reanalysis reference is the standard methodological choice.

S2 Autocorrelation Adjustment and Trend Estimation

Temperature trends were estimated using the Modified Mann-Kendall (MMK) test (Hamed and Ramachandra Rao 1998) and Sen's slope estimator (Sen 1968), implemented via the *mmkh* function in the *modifiedmk* R package. The MMK test extends the standard Mann-Kendall test by adjusting the variance of the test statistic to account for serial autocorrelation, thereby avoiding false detection of significant trends. The original Mann-Kendall (MK) test statistic S is defined as:

$$S = \sum_{i=1}^{n-1} \sum_{j=i+1}^{n} \operatorname{sgn}(x_j - x_i) \tag{9}$$

where n is the number of data points, x_i and x_j are the sequential data values, and the sign function $\operatorname{sgn}(x_j - x_i)$ is given by:

$$\operatorname{sgn}(x_j - x_i) = \begin{cases} 1 & \text{if } (x_j - x_i) > 0 \\ 0 & \text{if } (x_j - x_i) = 0 \\ -1 & \text{if } (x_j - x_i) < 0 \end{cases} \tag{10}$$

For datasets where $n > 10$, the variance of S is calculated to determine the standardised test statistic Z:

$$\operatorname{Var}(S) = \frac{n(n-1)(2n+5) - \sum_{k=1}^{m} t_k(t_k - 1)(2t_k + 5)}{18} \tag{11}$$

where m is the number of linked groups and t_k is the number of data points in the k^{th} group. The standardised statistic Z follows a normal distribution:

$$Z = \begin{cases} \dfrac{S-1}{\sqrt{\operatorname{Var}(S)}} & \text{if } S > 0 \\ 0 & \text{if } S = 0 \\ \dfrac{S+1}{\sqrt{\operatorname{Var}(S)}} & \text{if } S < 0 \end{cases} \tag{12}$$

The MMK test addresses serial autocorrelation by adjusting the variance to a corrected value $\operatorname{Var}^*(S)$:

$$\operatorname{Var}^*(S) = \operatorname{Var}(S) \cdot \frac{n}{n^*} = \operatorname{Var}(S) \left[1 + \frac{2}{n(n-1)(n-2)} \sum_{i=1}^{n-1} (n-i)(n-i-1)(n-i-2)\rho_i \right] \tag{13}$$

where ρ_i denotes the autocorrelation function of the ranks of the data. The magnitude and direction of trends were estimated using Sen's slope estimator, which is non-parametric, robust against outliers, and does not require normality (Sen 1968). All trend analyses were conducted at a 95% confidence level ($p < 0.05$).

S3 Satellite and Reanalysis Estimates

ERA5 Reanalysis

ERA5 (Hersbach et al. 2020; Bell et al. 2021) is ECMWF's fifth-generation global reanalysis, produced by ingesting observations from satellites, radiosondes, and surface stations into a 4D-Var data assimilation framework. We used the 2-metre temperature (T_{2m}) product at its native resolution of approximately 31 km. ERA5 has demonstrated skill in capturing broad temperature patterns and seasonal cycles over West Africa (Parsons et al. 2022).

CHIRTS-daily

CHIRTS-daily (Verdin et al. 2020) delivers daily Tmax and Tmin estimates at $0.05° \times 0.05°$ resolution. Monthly CHIRTSmax fields, derived by combining satellite thermal infrared retrievals with surface station data, are scaled to daily resolution using ERA5 as a temporal disaggregation reference; daily Tmin is then obtained by subtracting the ERA5 diurnal temperature range (DTR) from the resulting Tmax estimates (Verdin et al. 2020).

S4 Supplementary Figures

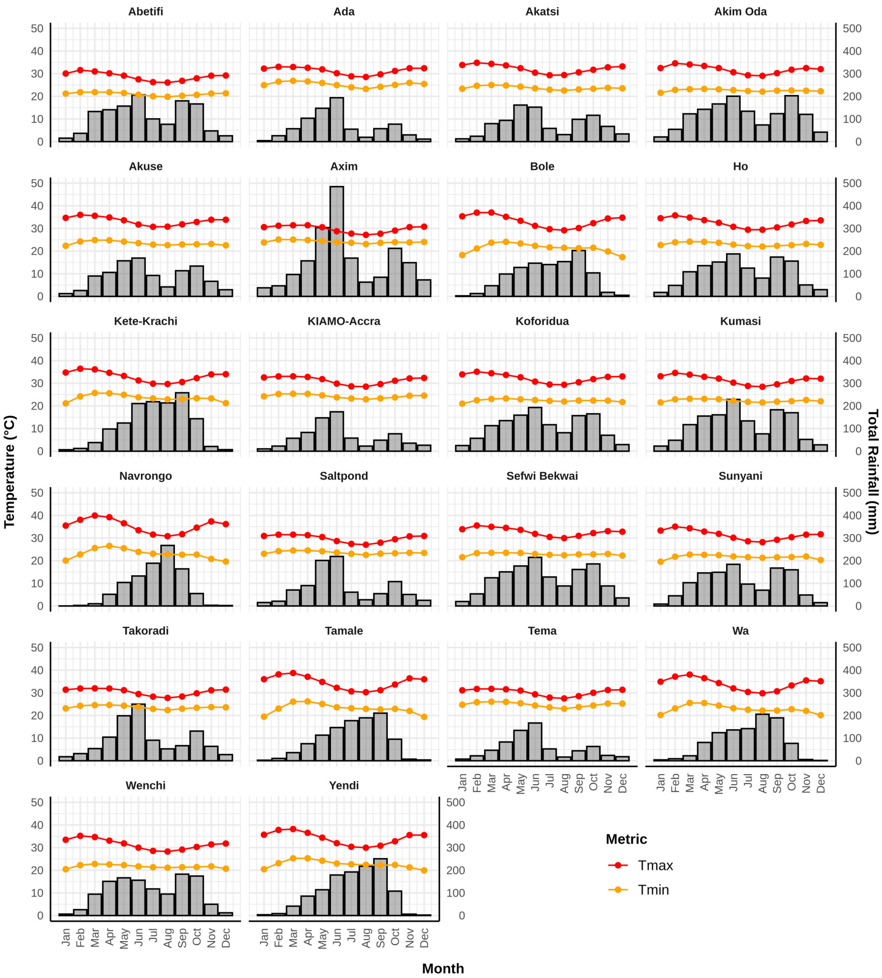

Fig. S5 Ombrothermic diagrams of the stations considered in the study. The bars show the mean monthly total rainfall values while the line plots show the mean Tmax (red) and mean Tmin (orange). The rainfall scale = temperature scale × 10.

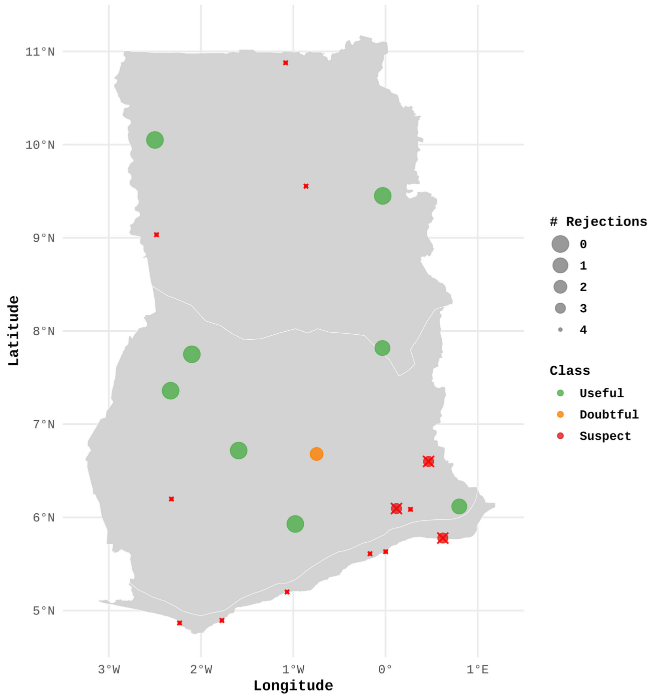

Fig. S6 A map showing the homogeneity test results for the annual DTR series across all stations. Green points represent Class A stations, orange Class B stations, while red points with an X on them represent Class C stations. The size of the points depicts, in the reverse order, the number of tests that rejected H_0.

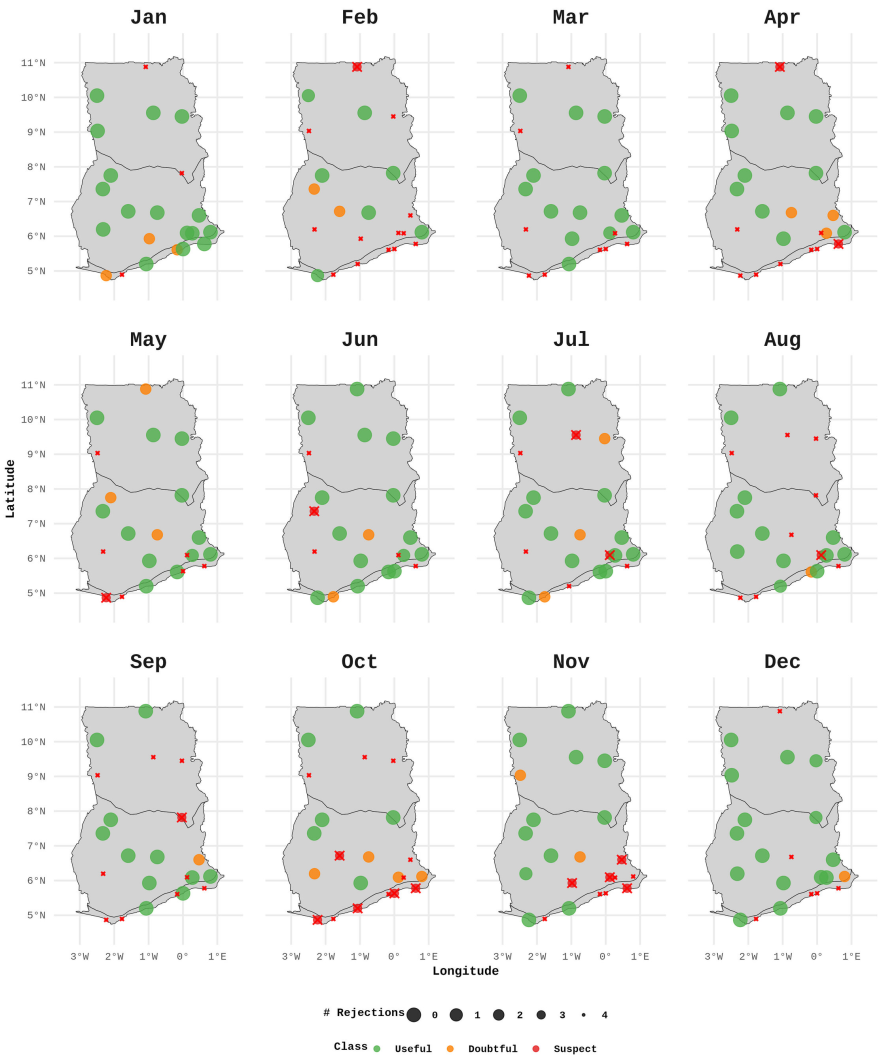

Fig. S7 A map showing the homogeneity test results for the monthly DTR series across all stations. Green points represent Class A stations, orange Class B stations, while red points with an X on them represent Class C stations. The size of the points depicts, in the reverse order, the number of tests that rejected H_0.

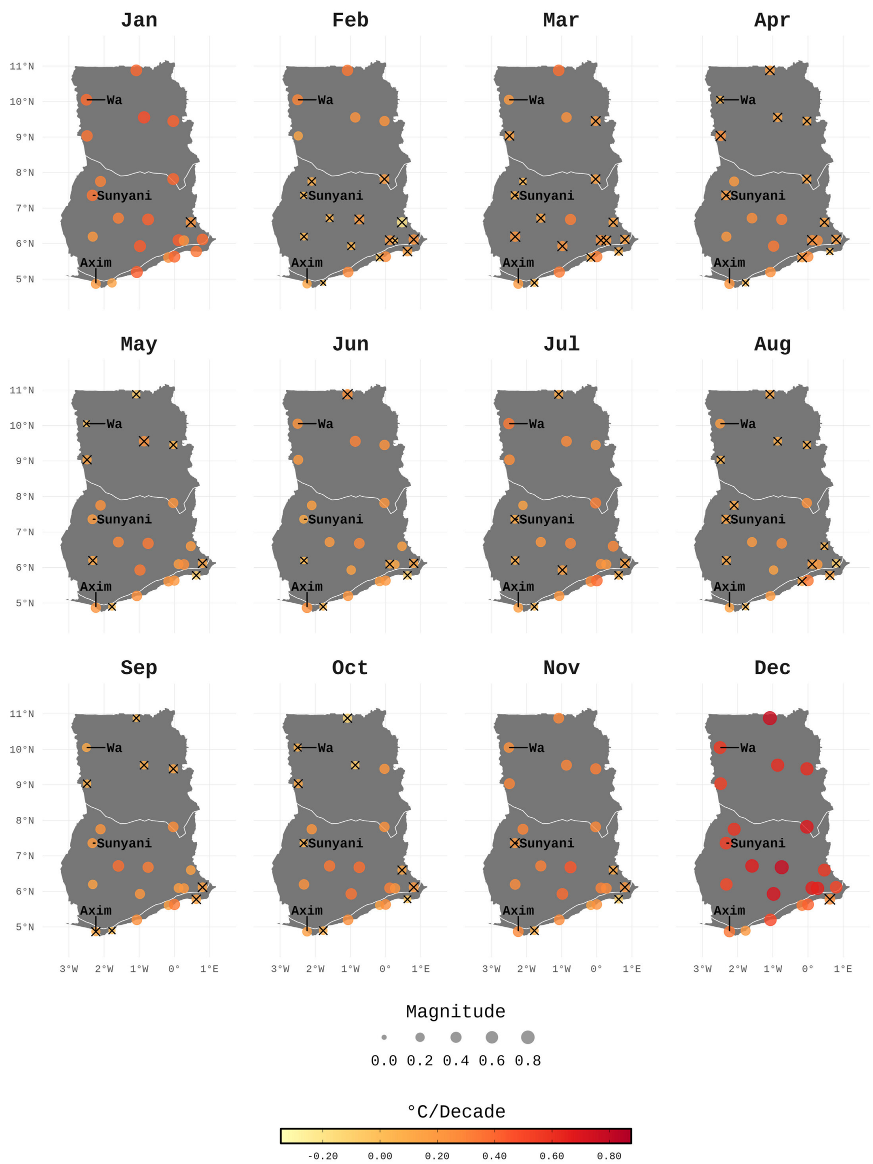

Fig. S8 Monthly spatial distribution of Tmax trends for all studied stations in Ghana. Each panel represents a calendar month. Point colour indicates the decadal warming rate (°C decade^{-1}), while point size reflects the absolute magnitude of change. Stations where the trend is not statistically significant ($p \geq 0.05$) are overlaid with a black cross (×).

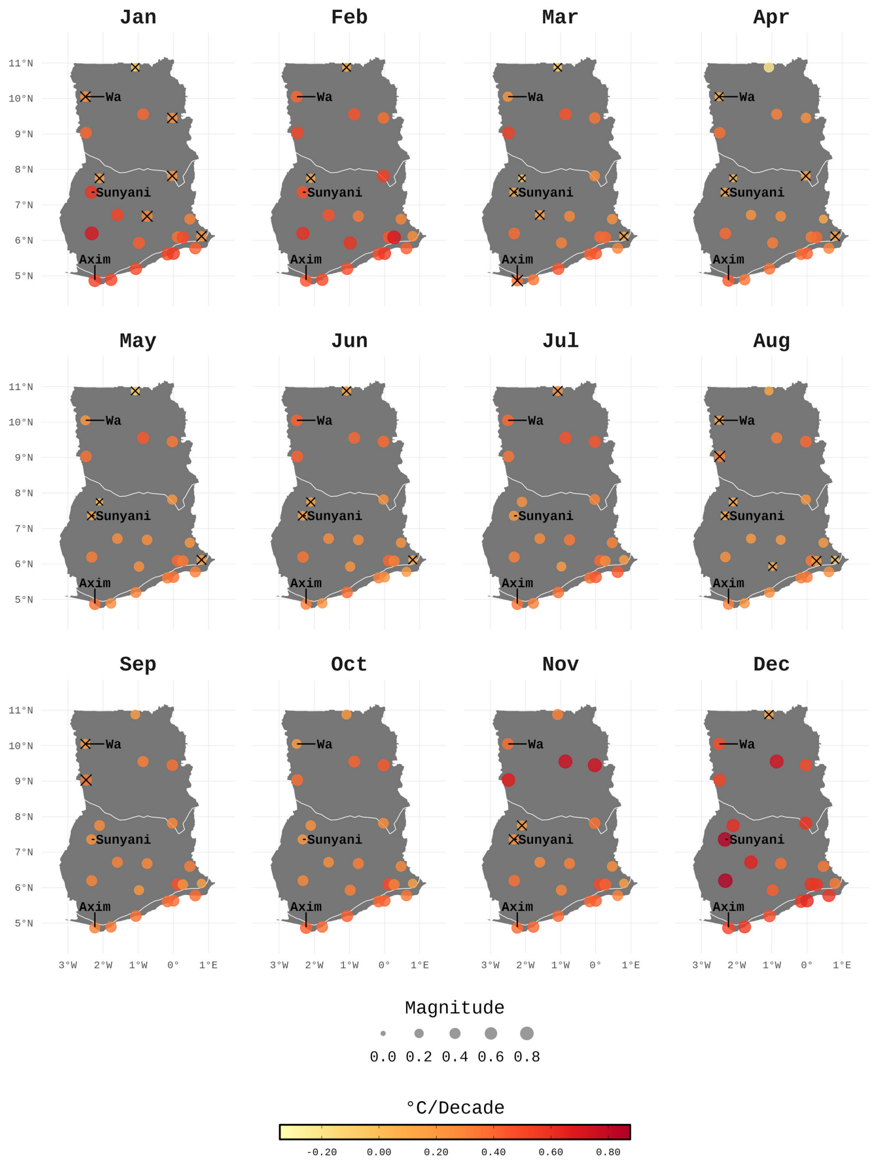

Fig. S9 Monthly spatial distribution of Tmin trends for all studied stations in Ghana, plotted similar to Fig. 8.

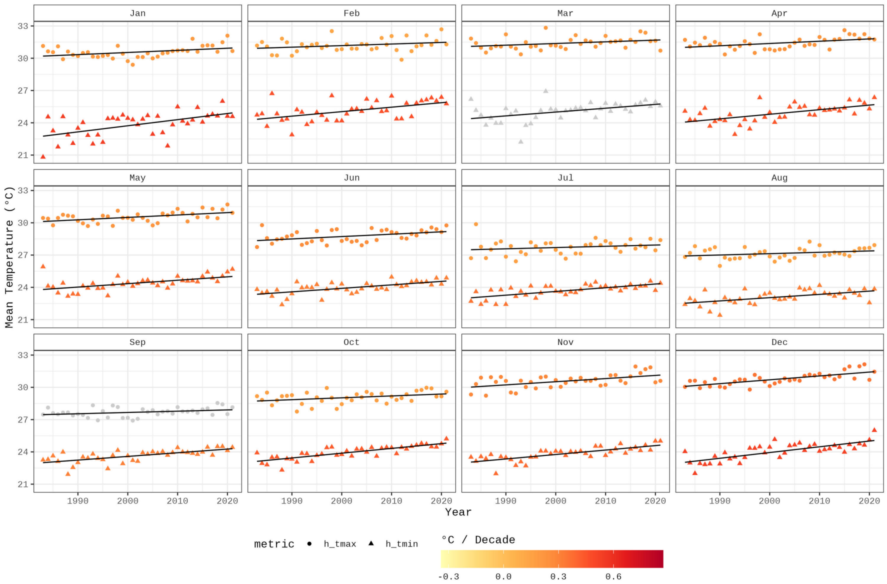

Fig. S10 Monthly distribution of Tmin and Tmax trends at Axim (coastal station). The y-axes represent mean Tmax (circles) and Tmin (triangles) while the x-axes represent the individual years. Grey symbols denote trends are not significant at $p < 0.05$. Black bar is the rate of change in °C decade^{-1}.

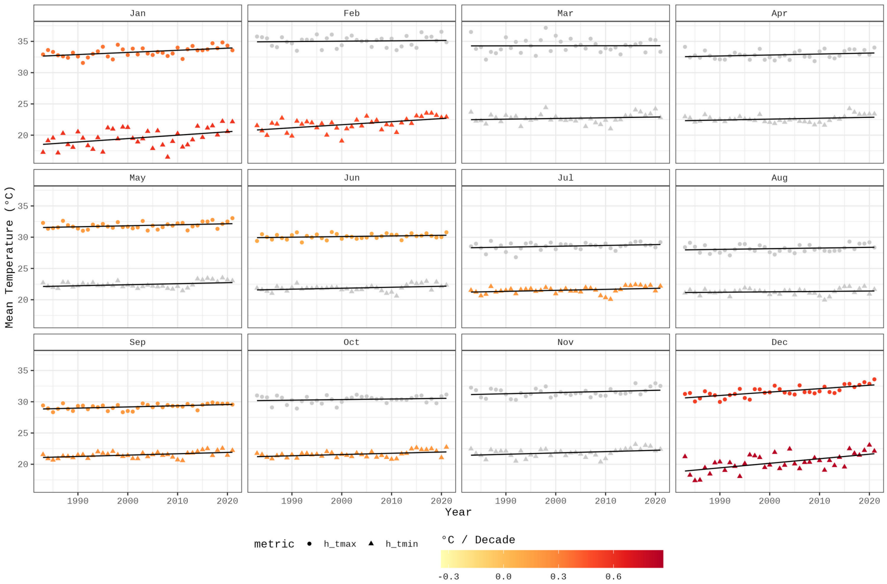

Fig. S11 Monthly distribution of Tmin and Tmax trends at Sunyani, plotted similar to Fig. 10.

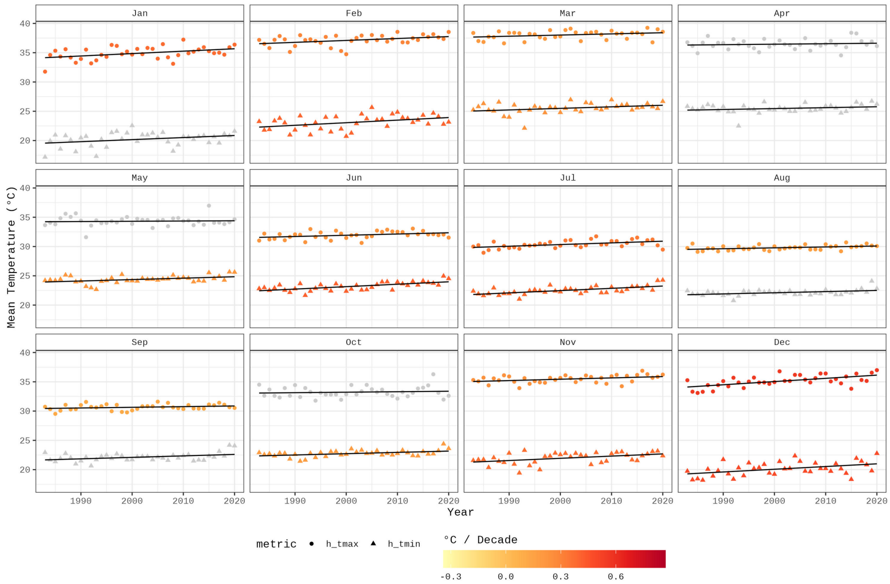

Fig. S12 Monthly distribution of Tmin and Tmax trends at Wa, plotted similar to Fig. 10.

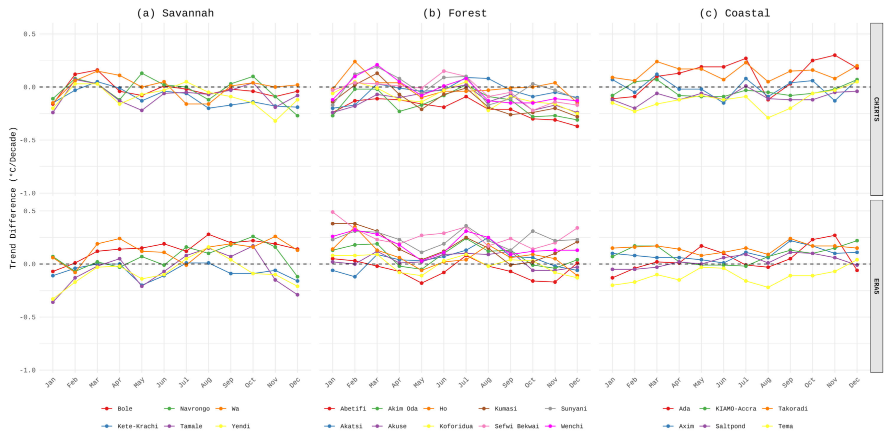

Fig. S13 Monthly Tmax trend differences (SRE minus observed, °C decade^{-1}) by climatic zone (a: Savannah, b: Forest, c: Coastal). Each line is a station; the dashed horizontal line marks zero difference. Rows: CHIRTS (top) and ERA5 (bottom).

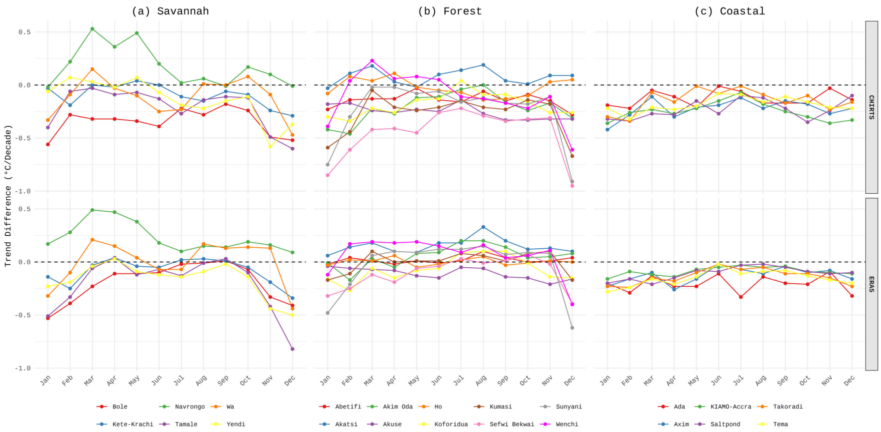

Fig. S14 Monthly Tmin trend differences (SRE minus observed, °C decade^{-1}) by climatic zone, plotted as in Fig. 13.

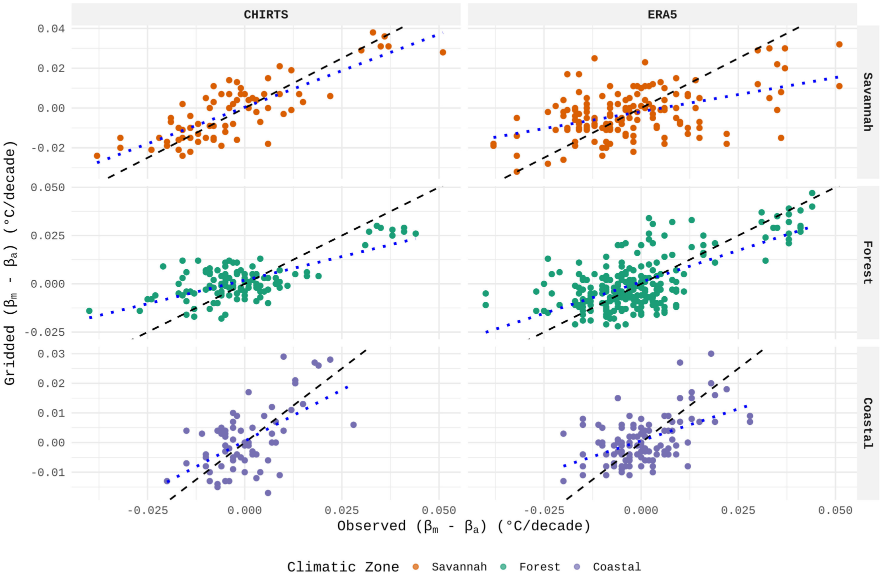

Fig. S15 Scatter plot of monthly Tmax trend deviations (observed vs. SRE) by climatic zone and SRE. The blue dotted lines represent the linear regression lines, and the black dashed lines indicate the 1:1 line. Each point represents a pair of monthly trend deviations (observed and SRE) for a given station.

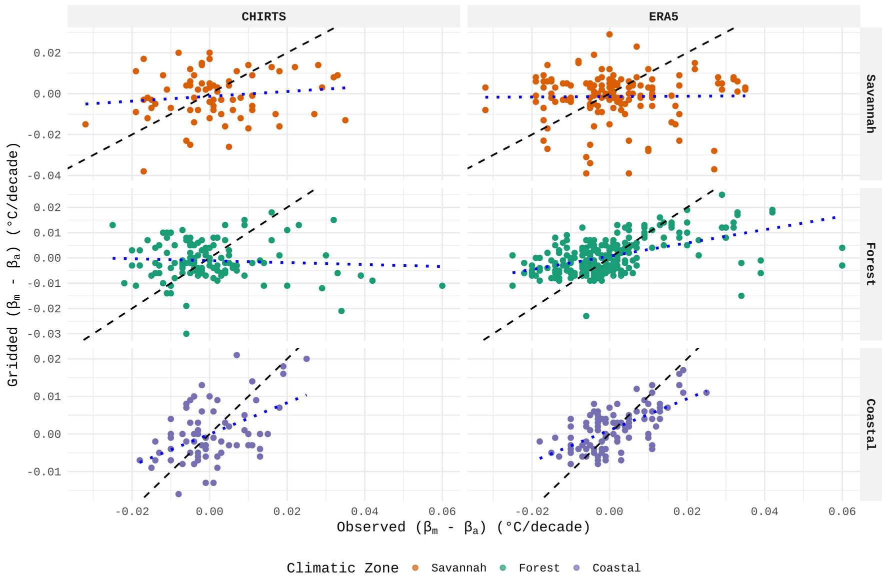

Fig. S16 Scatter plot of monthly Tmin trend deviations (observed vs. SRE) by climatic zone and SRE, plotted similar to Fig. 15.

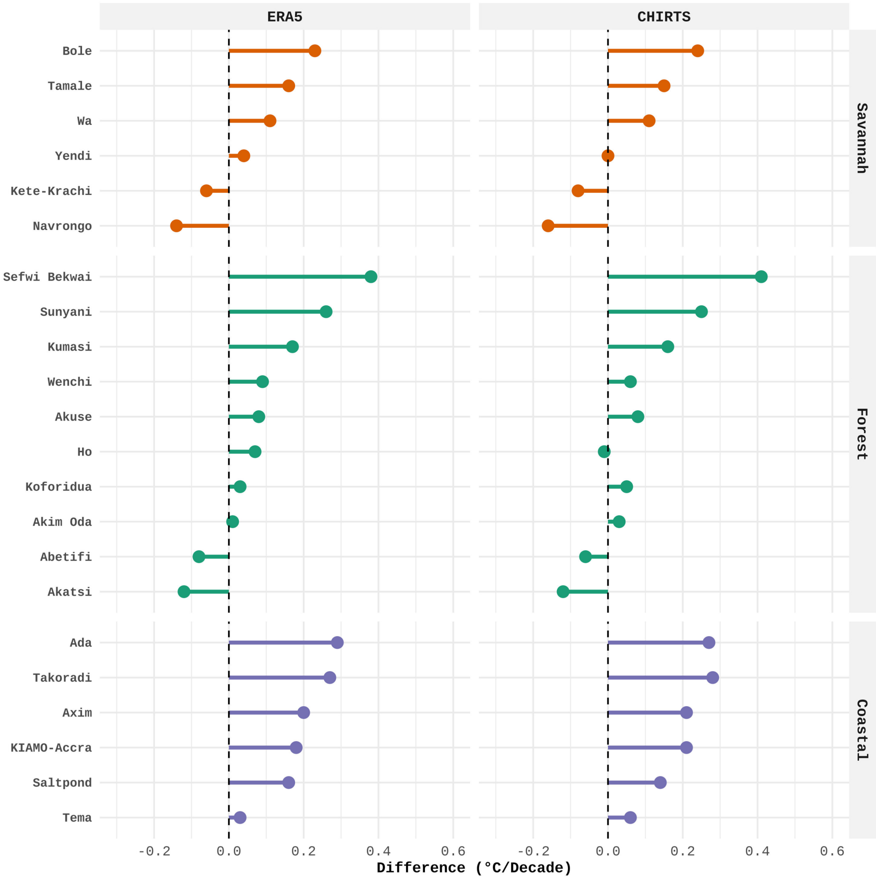

Fig. S17 Lollipop plots showing the differences in decadal DTR trends (SRE minus observed) across various stations in Ghana.

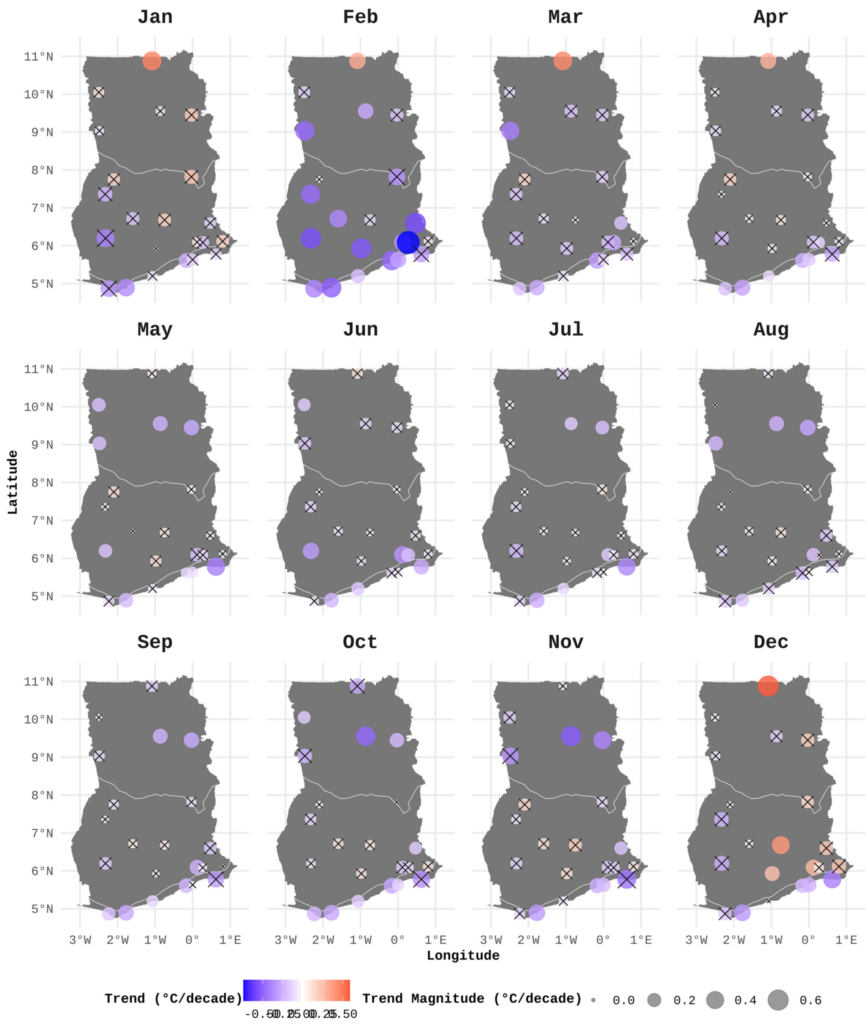

Fig. S18 Mean observed monthly DTR (homogenised) trends in Ghana. The colour gradient from blue (decreasing trends) through white (no trend) to red (increasing trends) indicates the trend value. Black X on a point indicates the trend at the location is not statistically significant ($p \geq 0.05$). Circle size is proportional to the absolute magnitude of the trend.

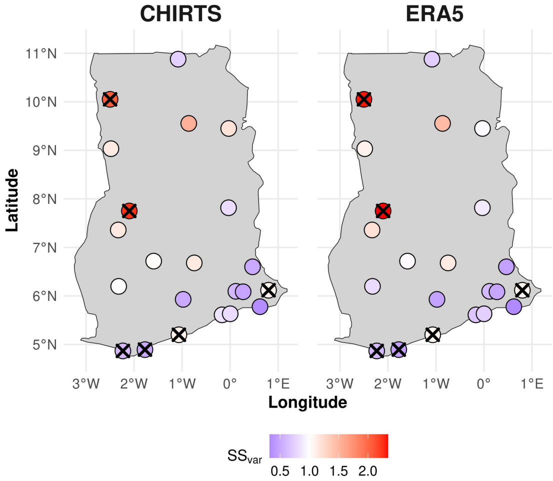

Fig. S19 Trend Variability Skill Score (SS_{var}) for DTR. Underestimation ($SS_{var} < 1$, blue), overestimation ($SS_{var} > 1$, red), white: similar variability with observed seasonal trends. Stations marked with a black cross ($\times$) have $STVI_{obs}$ below the first quartile of the DTR distribution (<0.009°C decade^{-1}) and their SS_{var} values should be interpreted with caution.

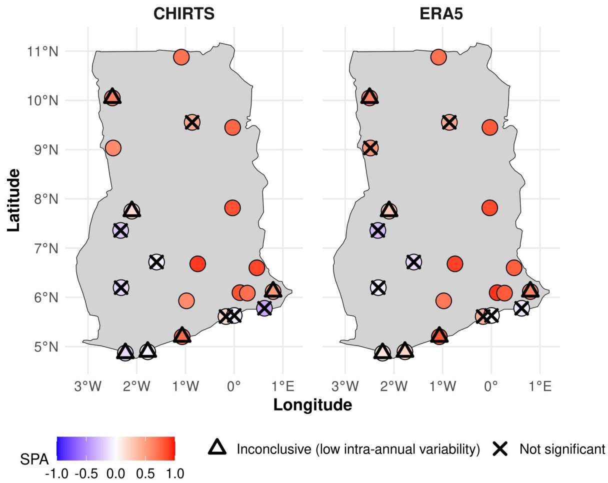

Fig. S20 Seasonal Phase Alignment (SPA) for DTR: Pearson correlation between observed and gridded monthly DTR trend deviations, plotted as in Fig. 6 of the main text. Stations marked with a black cross ($\times$) have $|SPA| < 0.576$ ($p < 0.05$, two-tailed, $N = 12$) and have sufficient intra-annual variability but are not statistically significant. Stations marked with a black triangle have $STVI_{obs}$ below the first quartile of the DTR distribution and have limited intra-annual variability, so SPA is not evaluated regardless of its value (Table S1).

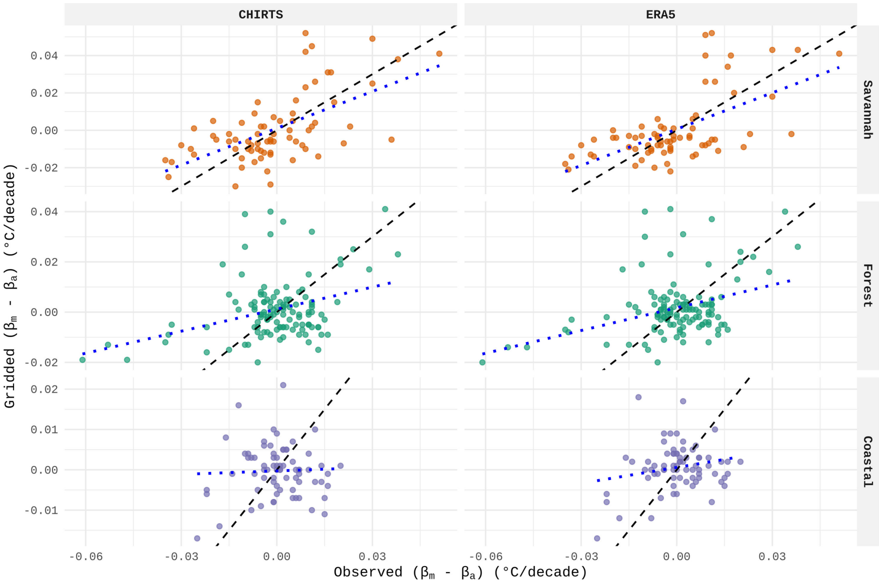

Fig. S21 Scatter plot of monthly DTR trend deviations (observed vs. SRE) by climatic zone and SRE.

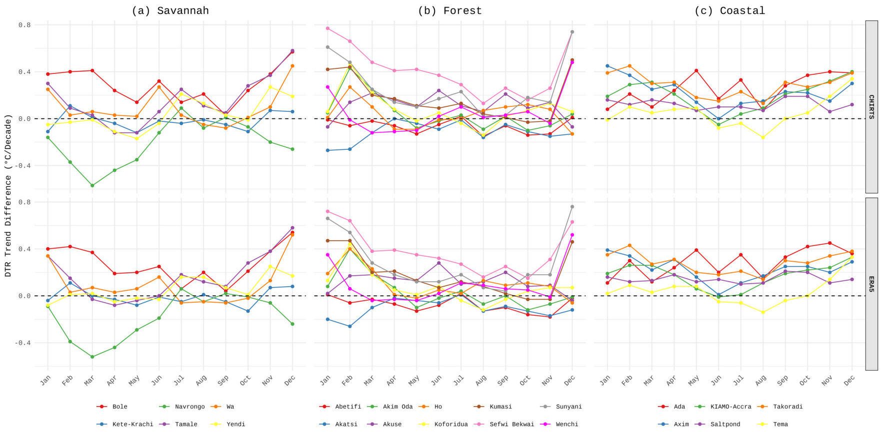

Fig. S22 Monthly DTR trend differences (SRE minus observed, °C decade^{-1}) by climatic zone (1983–2021), plotted as in Fig. 13. Positive biases of 0.1–0.4°C decade^{-1} prevailed in the Coastal zone and 0.3–0.9°C decade^{-1} in the Forest zone during dry season months. Navrongo (Savannah) showed contrasting large negative biases from December to May.

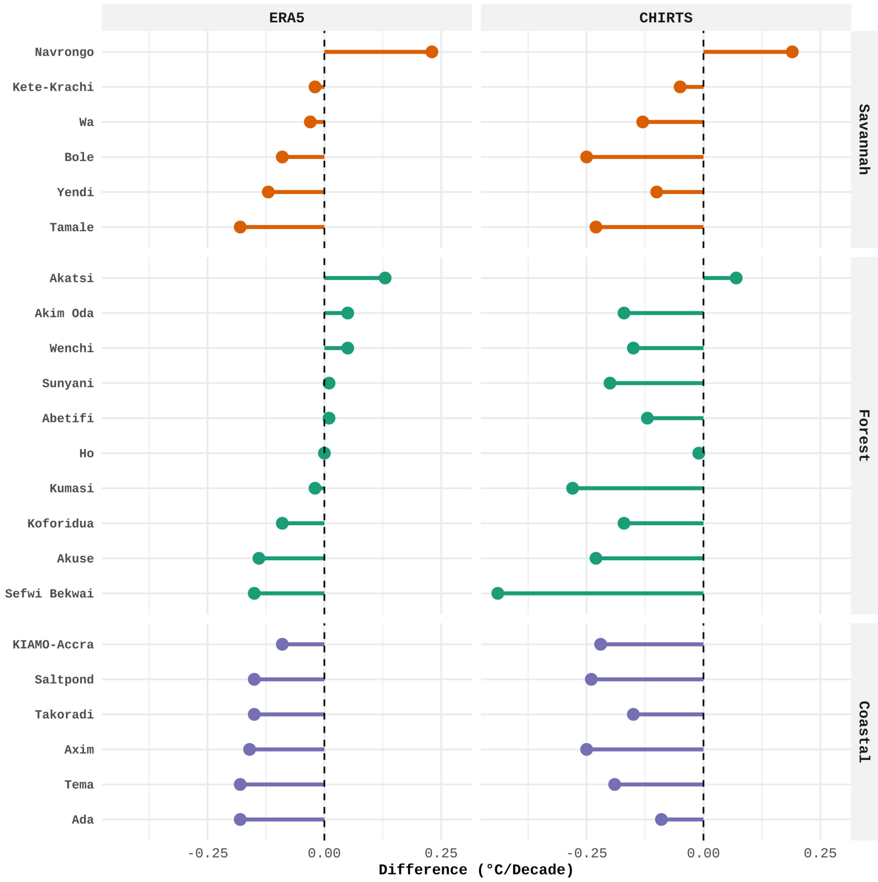

Fig. S23 Lollipop plots showing the differences in decadal Tmin trends (gridded minus observed) across the 22 stations in Ghana, plotted in a similar fashion as Fig. 3 of the main text.

S5 Supplementary Tables

Table S1 Classification of SPA values by intra-annual variability. Stations with $STVI_{obs}$ below the first quartile (Q1) of its observed distribution have too little genuine intra-annual trend signal for SPA to be conclusive and are classified as having limited variability regardless of their SPA value; among the remaining (”sufficient-variability”) stations, SPA is classified as significant or not significant against the $p < 0.05$ critical value ($|\text{SPA}| \geq 0.576$, $N = 12$, two-tailed).

Variable	Product	Sufficient variability	Genuine sig.	Genuine non-sig.	Insufficient variability	% genuine sig.[a]
Tmax	ERA5	16/22	9	7	6	56%
Tmax	CHIRTS	16/22	13	3	6	81%
Tmin	ERA5	16/22	8	8	6	50%
Tmin	CHIRTS	16/22	6	10	6	38%
DTR	ERA5	16/22	8	8	6	50%
DTR	CHIRTS	16/22	9	7	6	56%

[a] Percentage of the 16 stations with sufficient intra-annual variability for which the SRE’s SPA value was statistically significant. Full station-level classification is given in Table S2.

Table S2 Station-level classification of SPA outcomes for each variable and product. S = genuine, significant ($STVI_{obs}$ above the first quartile (Q1) and $|SPA| \geq 0.576$); N = genuine, not significant ($STVI_{obs}$ above Q1 and $|SPA| < 0.576$); I = insufficient variability ($STVI_{obs}$ below Q1 of its distribution, regardless of SPA). See Table S1 for summary counts and Sect. 2.6 of the main text for metric definitions.

		Tmax		Tmin		DTR	
Station	Zone	ERA5	CHIRTS	ERA5	CHIRTS	ERA5	CHIRTS
Ada	Coastal	N	N	S	S	N	N
Axim	Coastal	I	I	I	I	I	I
KIAMO-Accra	Coastal	I	I	I	I	N	N
Saltpond	Coastal	I	I	I	I	I	I
Takoradi	Coastal	I	I	S	N	I	I
Tema	Coastal	I	I	S	S	N	N
Abetifi	Forest	S	S	I	I	S	S
Akatsi	Forest	S	S	S	S	I	I
Akim Oda	Forest	S	S	S	N	S	S
Akuse	Forest	S	S	I	I	S	S
Ho	Forest	N	S	I	I	S	S
Koforidua	Forest	S	S	S	S	S	S
Kumasi	Forest	N	N	S	S	N	N
Sefwi Bekwai	Forest	I	I	S	N	N	N
Sunyani	Forest	S	S	N	N	N	N
Wenchi	Forest	S	N	N	N	I	I
Bole	Savannah	N	S	N	N	N	S
Kete-Krachi	Savannah	S	S	N	S	S	S
Navrongo	Savannah	S	S	N	N	S	S
Tamale	Savannah	N	S	N	N	N	N
Wa	Savannah	N	S	N	N	I	I
Yendi	Savannah	N	S	N	N	S	S

Table S3 Homogeneity test results for the annual DTR series across all stations. Values represent test statistics and associated p-values

Station	U (PT)	p (PT)	T (SNHT)	p (SNHT)	V (BLRT)	p (BLRT)	U (BUT)	p (BUT)	Rejects	Class
Abetifi	87	0.263	13.870	0.0004	0.692	0.0007	0.255	0.182	2	B
Ada	103	0.024	8.091	0.0345	0.569	0.0351	0.435	0.052	3	C
Akatsi	124	0.051	6.745	0.0930	0.474	0.0954	0.457	0.046	1	A
Akim Oda	117	0.054	6.663	0.0962	0.479	0.0950	0.341	0.102	0	A
Akuse	88	0.162	17.150	5.0e-5	0.796	1.0e-4	0.468	0.045	3	C
Axim	140	0.002	11.483	0.0027	0.652	0.0032	0.951	0.002	4	C
Bole	132	0.010	15.243	1.0e-4	0.738	1.0e-4	0.734	0.007	4	C
Ho	102	0.127	11.016	0.0044	0.616	0.0049	0.473	0.039	3	C
KIAMO-Accra	185	0.000	16.822	0.0000	0.762	5.0e-5	1.810	0.000	4	C
Kete-Krachi	122	0.041	6.187	0.1291	0.462	0.1227	0.279	0.152	1	A
Koforidua	154	0.012	8.062	0.0445	0.510	0.0436	0.639	0.014	4	C
Kumasi	97	0.352	3.016	0.6173	0.302	0.6053	0.148	0.405	0	A
Navrongo	146	0.030	10.642	0.0088	0.577	0.0093	0.705	0.010	4	C
Saltpond	140	0.029	9.448	0.0196	0.552	0.0188	0.661	0.012	4	C
Sefwi Bekwai	146	0.011	10.773	0.0064	0.599	0.0071	0.585	0.022	4	C
Sunyani	104	0.231	6.010	0.1470	0.433	0.1488	0.138	0.443	0	A
Takoradi	182	1.0e-4	14.600	2.0e-4	0.721	5.0e-5	1.584	0.000	4	C
Tamale	156	1.0e-4	15.600	5.0e-5	0.774	1.0e-4	1.501	0.000	4	C
Tema	265	0.000	17.819	5.0e-5	0.735	1.0e-4	1.000	0.001	4	C
Wa	68	0.657	2.856	0.6375	0.304	0.6398	0.106	0.572	0	A
Wenchi	52	0.101	2.734	0.5937	0.390	0.5976	0.183	0.314	0	A
Yendi	74	0.112	5.343	0.1728	0.482	0.1752	0.255	0.181	0	A

References

Alexandersson, H.: A homogeneity test applied to precipitation data. Journal of climatology **6**(6), 661–675 (1986)

Bell, B., Hersbach, H., Simmons, A., Berrisford, P., Dahlgren, P., Horányi, A., Muñoz-Sabater, J., Nicolas, J., Radu, R., Schepers, D., Soci, C., Villaume, S., Bidlot, J., Haimberger, L., Woollen, J., Buontempo, C., Thépaut, J.: The ERA5 global reanalysis: Preliminary extension to 1950. Quarterly Journal of the Royal Meteorological Society **147**(741), 4186–4227 (2021) https://doi.org/10.1002/qj.4174

Buishand, T.A.: Tests for detecting a shift in the mean of hydrological time series. Journal of Hydrology **73**(1–2), 51–69 (1984) https://doi.org/10.1016/0022-1694(84)90032-5

Copernicus Climate Change Service: Agrometeorological indicators from 1979 up to 2019 derived from reanalysis. ECMWF (2019). https://doi.org/10.24381/CDS.6C68C9BB . https://cds.climate.copernicus.eu/doi/10.24381/cds.6c68c9bb

Guijarro, J.A.: Climatol: Climate Tools (Series Homogenization and Derived Products). (2025). R package version 4.4-0. https://CRAN.R-project.org/package=climatol

Hersbach, H., Bell, B., Berrisford, P., Hirahara, S., Horányi, A., Muñoz-Sabater, J., Nicolas, J., Peubey, C., Radu, R., Schepers, D., Simmons, A., Soci, C., Abdalla, S., Abellan, X., Balsamo, G., Bechtold, P., Biavati, G., Bidlot, J., Bonavita, M., Chiara, G., Dahlgren, P., Dee, D., Diamantakis, M., Dragani, R., Flemming, J., Forbes, R., Fuentes, M., Geer, A., Haimberger, L., Healy, S., Hogan, R.J., Hólm, E., Janisková, M., Keeley, S., Laloyaux, P., Lopez, P., Lupu, C., Radnoti, G., Rosnay, P., Rozum, I., Vamborg, F., Villaume, S., Thépaut, J.-N.: The ERA5 global reanalysis. Quarterly Journal of the Royal Meteorological Society **146**(730), 1999–2049 (2020) https://doi.org/10.1002/qj.3803

Hamed, K.H., Ramachandra Rao, A.: A modified Mann-Kendall trend test for autocorrelated data. Journal of Hydrology **204**(1–4), 182–196 (1998) https://doi.org/10.1016/s0022-1694(97)00125-x

Pettitt, A.N.: A non-parametric approach to the change-point problem. Journal of the Royal Statistical Society: Series C (Applied Statistics) **28**(2), 126–135 (1979)

Parsons, D., Stern, D., Ndanguza, D., Sylla, M.B.: Evaluation of satellite-based air temperature estimates at eight diverse sites in Africa. Climate **10**(7) (2022) https://doi.org/10.3390/cli10070098

Sen, P.K.: Estimates of the regression coefficient based on Kendall's Tau. Journal of the American Statistical Association **63**(324), 1379–1389 (1968) https://doi.org/10.1080/01621459.1968.10480934

Verdin, A., Funk, C., Peterson, P., Landsfeld, M., Tuholske, C., Grace, K.: Development and validation of the CHIRTS-daily quasi-global high-resolution daily temperature data set. Scientific Data **7**(1), 303 (2020)

Wijngaard, J., Klein Tank, A., Können, G.: Homogeneity of 20th century European daily temperature and precipitation series. International Journal of Climatology: A Journal of the Royal Meteorological Society **23**(6), 679–692 (2003)

World Meteorological Organization: Guidelines on Surface Station Data Quality Control and Quality Assurance for Climate Applications. World Meteorological Organization, Geneva, Switzerland (2021). WMO-No. 1269